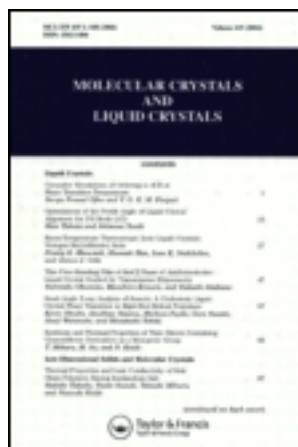


This article was downloaded by: [Tomsk State University of Control Systems and Radio]

On: 20 February 2013, At: 11:55

Publisher: Taylor & Francis

Informa Ltd Registered in England and Wales Registered Number: 1072954  
Registered office: Mortimer House, 37-41 Mortimer Street, London W1T 3JH, UK



## Molecular Crystals and Liquid Crystals

Publication details, including instructions for authors and subscription information:

<http://www.tandfonline.com/loi/gmcl16>

### Inductive And Resistive Studies Of The Ambient Pressure Organic Superconductor $\beta$ -(BEDT-TTF) $_2$ I $_3$

K. Douglas Carlson<sup>a</sup>, G. W. Crabtree<sup>a</sup>, M. Choi<sup>a</sup>, L. N. Hall<sup>a</sup>, P. Thomas Copps<sup>a</sup>, Hau H. Wang<sup>a</sup>, Thomas J. Emge<sup>a</sup>, Mark A. Beno<sup>a</sup> & Jack M. Williams<sup>a</sup>

<sup>a</sup> Chemistry and Materials Science and Technology Divisions, Argonne National Laboratory, Argonne, Illinois, 60439

Version of record first published: 17 Oct 2011.

To cite this article: K. Douglas Carlson, G. W. Crabtree, M. Choi, L. N. Hall, P. Thomas Copps, Hau H. Wang, Thomas J. Emge, Mark A. Beno & Jack M. Williams (1985): Inductive And Resistive Studies Of The Ambient Pressure Organic Superconductor  $\beta$ -(BEDT-TTF) $_2$ I $_3$ , Molecular Crystals and Liquid Crystals, 125:1, 145-158

To link to this article: <http://dx.doi.org/10.1080/00268948508080095>

PLEASE SCROLL DOWN FOR ARTICLE

Full terms and conditions of use: <http://www.tandfonline.com/page/terms-and-conditions>

This article may be used for research, teaching, and private study purposes. Any substantial or systematic reproduction, redistribution, reselling, loan,

sub-licensing, systematic supply, or distribution in any form to anyone is expressly forbidden.

The publisher does not give any warranty express or implied or make any representation that the contents will be complete or accurate or up to date. The accuracy of any instructions, formulae, and drug doses should be independently verified with primary sources. The publisher shall not be liable for any loss, actions, claims, proceedings, demand, or costs or damages whatsoever or howsoever caused arising directly or indirectly in connection with or arising out of the use of this material.

## INDUCTIVE AND RESISTIVE STUDIES OF THE AMBIENT PRESSURE ORGANIC SUPERCONDUCTOR $\beta$ -(BEDT-TTF) $_2$ I $_3$

K. DOUGLAS CARLSON, G. W. CRABTREE, M. CHOI,  
L. N. HALL, P. THOMAS COPPS, HAU H. WANG, THOMAS J.  
EMGE, MARK A. BENO AND JACK M. WILLIAMS

Chemistry and Materials Science and Technology  
Divisions, Argonne National Laboratory, Argonne,  
Illinois 60439

**Abstract** Inductive studies based on rf penetration depth measurements and resistive studies based on 4-lead electrical resistivity measurements are reported for the sulfur-based ambient pressure superconductor  $\beta$ -(BEDT-TTF) $_2$ I $_3$ . The inductive studies show that the bulk superconducting transition temperature ( $T_c$ ) is sample dependent, with values of  $T_c$  ranging from 1.2 K to 1.4 K. The critical magnetic fields  $H_{c2}$  show considerable anisotropy in directions perpendicular and parallel to the crystallographic *ab* plane. The electrical resistivity as a function of temperature shows linear and quadratic dependences on  $T$  and unusual structure near 8 K and 4 K.

### INTRODUCTION

The discovery<sup>1</sup> in 1980 of superconductivity in the Bechgaard salts, (TMTSF) $_2$ X, where TMTSF is the Se-based organic radical-cation donor tetramethyltetraselenafulvalene and X is a univalent complex inorganic anion, has stimulated the search for new organic conductors having a superconducting state. These TMTSF salts constitute the first known class of organic superconductors. Charge-transfer salts of the type (BEDT-TTF) $_2$ X, derived from the

BEDT-TTF donor bis(ethylenedithio)tetrathiafulvalene, abbreviated as "ET", now constitute the second class of organic superconductors, with potentially more interesting normal-state and superconducting properties than the TMTSF derivatives. Parkin *et al.*<sup>2</sup> first discovered superconductivity in these S-based organic conductors in studies of  $(\text{ET})_2\text{ReO}_4$ , which was reported to be superconducting near 2 K at pressures above 4 kbar. Yagubskii *et al.*<sup>3</sup> first discovered ambient pressure superconductivity in the ET salts with the  $\text{I}_3^-$  anionic derivative,  $\beta-(\text{ET})_2\text{I}_3$ , which was reported to be superconducting at 1.4-1.5 K. This discovery of ambient pressure superconductivity, second only to  $(\text{TMTSF})_2\text{ClO}_4$ , has since been confirmed to be a volume (bulk) property of  $\beta-(\text{ET})_2\text{I}_3$ .<sup>4-7</sup> Although the existence of a superconducting state is now well documented for  $\beta-(\text{ET})_2\text{I}_3$ , the various normal-state and superconducting properties of this salt remain largely uncharacterized. In this article, we describe inductive and resistive studies at ambient pressure of  $\beta-(\text{ET})_2\text{I}_3$  which focus on (1) variations in the onset temperature of bulk superconductivity, (2) the anisotropy in the upper critical magnetic fields, (3) the temperature dependence of the electrical resistivity, and (4) the resistivity near 200 K where the crystals undergo a novel transition to an incommensurate modulated structure.<sup>8-9</sup>

#### EXPERIMENTAL PROCEDURES

$\beta-(\text{ET})_2\text{I}_3$  crystals were prepared by electrochemical oxidation of ET (*i.e.*, BEDT-TTF) in the presence of the supporting electrolyte  $(n\text{-Bu}_4\text{N})\text{I}_3$ , as previously described.<sup>4</sup> The electrocrystallization produced at least

two phases: the nonsuperconducting  $\alpha$ -(ET) $_2$ I $_3$  phase, which has a metal-insulator transition near 140 K,<sup>10</sup> and the superconducting  $\beta$ -(ET) $_2$ I $_3$  phase (both with space group P $\bar{1}$ ,  $Z = 1$ ). The  $\beta$  phase involves stacks of the ET molecules interconnected by S...S contact distances (interstack distances) which are less than the van der Waals S-atom radius sum (3.60 Å).<sup>4</sup> This arrangement produces a corrugated-sheet network of S-atoms which promotes electrical conductivity in the crystallographic ab plane. Depending on the solvent and other parameters, the electrocrystallization produces both  $\alpha$  and  $\beta$  phases and several crystal morphologies. Prominent among the  $\beta$  phase morphologies are distorted hexagon-shaped<sup>4</sup> crystals and needlelike<sup>3</sup> crystals.

The inductive studies discussed in this article were carried out on two kinds of samples consisting of roughly hexagon-shaped crystals. One sample consisted of a single  $\beta$ -phase crystal with dimensions of  $\sim 1 \times 1 \times 0.3$  mm<sup>3</sup>. The other sample consisted of a mixture of smaller  $\beta$ -phase crystals, each with dimensions of  $\sim 0.5 \times 0.2 \times 0.05$  mm<sup>3</sup> or smaller. The small crystals were taken from a different electrocrystallization synthesis than that of the large single-crystal specimen. The inductive experiments consisted of rf penetration depth measurements<sup>11</sup> down to temperatures of  $\sim 0.4$ – $0.5$  K (pumped He<sup>3</sup>) in applied static magnetic fields in the range of 0–15 kOe. In this method, superconductivity is detected by an increase in the rf resonant frequency of an LC circuit due to the persistent shielding currents of a superconductor suspended in the rf coil. The rf frequency can be determined to  $\sim 1$  part in

$10^5$  Hz, which permits the detection of bulk superconductivity in as little as  $\sim 5 \mu\text{g}$  of a superconducting sample.<sup>5</sup> The resistive studies consisted of 4-lead electrical resistivity measurements<sup>12</sup> as a function of temperature on a needlelike crystal with dimensions of  $\sim 1.3 \times 0.1 \times 0.06 \text{ mm}^3$ . The leads were gold wires attached by conductive gold paste, and the measurements employed low-frequency ac currents ( $50 \mu\text{A}$  at 37 Hz) with phase-sensitive detection of the voltage. The resistivity was measured in the high-conductivity ab plane along the needle axis, which is the crystallographic a axis.

#### INDUCTIVE MEASUREMENTS BY RF PENETRATION

Several different definitions have been employed for the so-called critical temperature  $T_c$  of superconductivity in organic conductors. These include the "half-signal" definition,<sup>13</sup> in which  $T_c$  is taken as the temperature at the midpoint of the transition from the normal-state to the superconducting-state value of a given property, and the "extrapolated-signal" definition<sup>7</sup>, in which  $T_c$  is determined by the intersection of linear extrapolations of the superconducting- and normal-state data. In inductive measurements, we prefer to define  $T_c$  as the temperature at which the induced signal (e.g., the rf resonant frequency) first departs from the normal-state value since this measures the onset of bulk (volume) diamagnetic shielding currents in the sample. Organic superconductors in general have low transition temperatures and rather broad superconducting transitions, so that these different definitions of  $T_c$  give significantly different temperatures.

Different values of  $T_c$  (however they are defined) may arise from different measuring techniques. Electrical resistivity, for example, may be dominated by filamentary behavior, whereas inductive signals are responsive to changes in the bulk properties of the conduction electrons. We have suggested<sup>5</sup> that another source of discrepancy in inductive measurements on  $\beta$ -(ET) $_2$ I $_3$  may be the physical dimensions of the crystals because of the possibility of relatively large London penetration depths in organic superconductors. With a crystal dimension being comparable to the penetration depth, the apparent  $T_c$  would be smaller than the actual  $T_c$  due to the penetration of the rf field through most of the sample at temperatures near  $T_c$ . The importance of this effect can be evaluated by comparing the values of  $T_c$  observed for a large and a small crystal.

Figure 1 shows the superconducting transition curves at zero applied magnetic field for the single crystal specimen of  $\beta$ -(ET) $_2$ I $_3$  and the polycrystalline sample. Both curves are broad and incomplete down to the lowest temperature achieved. The difference in signal size is attributed to the difference in volumes of the two samples. The curve for the polycrystalline sample, with  $T_c = 1.40 \pm 0.02$  K for the onset of bulk superconductivity, has been reported previously.<sup>5</sup> The curve for the single crystal specimen has  $T_c = 1.23 \pm 0.02$  K, which is considerably smaller than the value for the polycrystalline sample even though the single crystal has much larger dimensions. In both experiments, the cooling rates were

comparable (overnight cooling from room temperature to  $\sim 70$  K and further cooling to  $\sim 2$  K at a rate of  $\sim 1$  K/m). This demonstrates that the penetration depth is not an especially important parameter for the crystals of  $\beta$ -(ET) $_2$ I $_3$  and that  $T_c$  is a sample dependent property. We have measured  $T_c \approx 1.30 \pm 0.02$  K in another sample of polycrystalline material. The largest  $T_c$  reported<sup>6</sup> to date for an inductive measurement (low-field ESR) on  $\beta$ -(ET) $_2$ I $_3$  is 1.6 K.

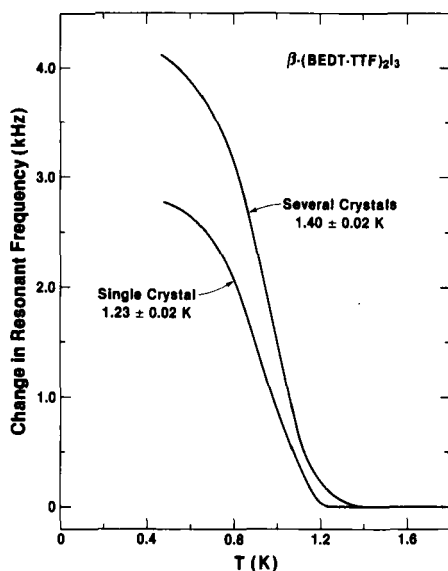


FIGURE 1. Change in rf resonant frequency vs temperature for two  $\beta$ -(BEDT-TTF) $_2$ I $_3$  samples at zero applied magnetic field.

Critical magnetic fields of the single-crystal  $\beta$ -(ET) $_2$ I $_3$  specimen were investigated by rf penetration depth measurements in fields applied along various orientations of the crystallographic axes. At fields near

$H = 0$  in all orientations, there was a sharp decrease in the oscillation frequency with the first application of the magnetic field, consistent with the measurements by Schwenk et al.<sup>7</sup> of very low values of  $H_{c1}$  ( $< 0.36$  Oe) for all three crystallographic axes. The oscillation frequency decreased smoothly with increasing field down to the resonant frequency of the normal state at  $H_{c2}$ . At temperatures near 1 K,  $H_{c2}(\parallel c^*)$  was  $\sim 400$  Oe for fields directed along the  $c^*$  axis, and  $H_{c2}(\perp c^*)$ , i.e., for  $H$  in the  $ab$  plane, was larger by more than an order-of-magnitude for fields parallel to the  $ab$  plane. The anisotropy of the critical fields was considerably smaller in the  $ab$  plane, thus confirming the two-dimensional metallic character of  $\beta$ -(ET)<sub>2</sub>I<sub>3</sub>. In a previous article,<sup>5</sup> we reported upper critical fields of  $\sim 600$  Oe at 0.45 K for the polycrystalline sample. This critical field represents an average of crystal orientations with a rather small fraction of solid angles having large critical fields.

#### ELECTRICAL RESISTIVITY

The electrical resistivity of the  $\beta$ -(ET)<sub>2</sub>I<sub>3</sub> needle along the  $a$  axis is illustrated for the temperature range of 300–1.3 K in Figure 2. This crystal had a resistivity of  $\sim 0.1 \Omega \text{ cm}$  at 300 K and a residual resistivity ratio ( $\rho_{300}/\rho_{4.2}$ ) of  $\sim 450$ , comparable to values reported by Yagubskii et al.<sup>3</sup> This figure shows a slight but abrupt resistance jump near 210 K, similar to resistance jumps often observed in the resistivity of (TMTSF)<sub>2</sub>X salts.<sup>14</sup> The resistivity was linear in the temperature from 200 to 100 K, and it closely followed a  $T^2$  dependence from 100–10 K. It is interesting, and perhaps significant

because of the layered-type structure of  $\beta\text{-(ET)}_2\text{I}_3$ , that  $\text{TiS}_2$  (a prototypical layered structure) also has a resistivity proportional to  $T^2$  over a large temperature range encompassing this region.<sup>15</sup> A  $T^2$  dependence is usually associated with electron-electron scattering, whereas a linear temperature dependence implies

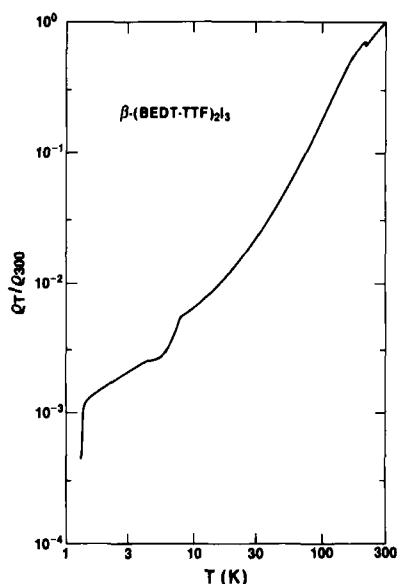


FIGURE 2. Log-log plot of the normalized resistivity ( $\rho_T/\rho_{300}$ ) along the needle axis (a axis) of  $\beta\text{-(BEDT-TTF)}_2\text{I}_3$  as a function of temperature.

electron-phonon scattering. Below 10 K, the resistivity shows an abrupt decrease near 8 K, suggestive of a first-order phase transition, and another decrease near 4 K.

These features are illustrated in Figure 3, and they are reproducible on thermal cycling of the crystal. This figure clearly illustrates the  $T^2$  dependence of the resistivity above  $\sim 10$  K.

Yagubskii et al.<sup>3</sup> reported that their needle-shaped crystals of  $\beta$ -(ET) $_2$ I $_3$  gave a decrease in resistivity near 4 K but their flakelike crystals (presumably like our hexagon-shaped crystals) exhibited only an insignificant decrease at this temperature. An examination of their graphical data shows a decrease in resistivity also near

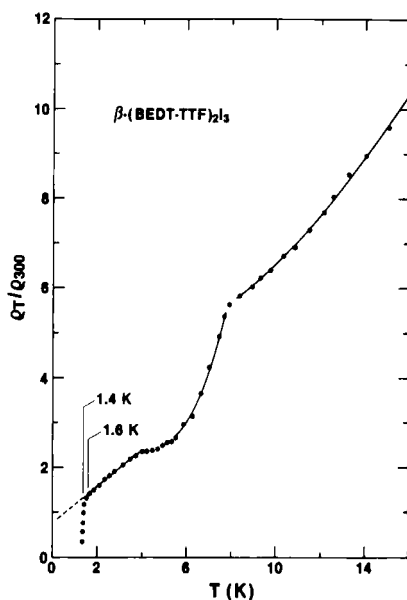


FIGURE 3. Normalized resistivity vs temperature of  $\beta$ -(BEDT-TTF) $_2$ I $_3$  from 16 K to 1.3 K. The solid curves are guides to the eye. The plotted points are selected values from a continuous graph of the sample resistance.

10 K for the needlelike crystals. We have explored this region by rf penetration depth measurements but have observed no change in the resonant frequency from the normal-state value from 12 K down to the bulk superconducting transition temperature. Figure 3 shows a nearly linear region of resistivity from 4 K to 1.6 K and a pronounced drop in resistivity beginning at 1.6 K with the "half-signal" resistivity occurring near 1.4 K, similar to the results reported by Yagubskii *et al.* These authors have shown that zero resistance occurs near 0.5 K, indicating that the superconducting transition is about as broad in resistivity measurements as it is in the inductive measurements.

The electrical resistivity behavior on thermal cycling of the needlelike crystal of  $\beta\text{-(ET)}_2\text{I}_3$  is illustrated in Figure 4. This behavior is quite similar to that described by Ishiguro *et al.*<sup>14</sup> for  $(\text{TMTSF})_2\text{ClO}_4$ . The curves labeled as 3 and 5 in Figure 4 represent, respectively, the third and fifth cooling and warming cycles between 300 K and 4.2 K or lower. The third cycle shows several sharp resistance jumps on cooling, one jump being rather large, and a somewhat smooth change in resistivity with the occurrence of a maximum near 150 K on warming. The initial cycle (not illustrated) gave much larger resistance jumps and a much larger maximum in the resistivity. The fifth cycle shows only one small resistance jump on cooling and a much smaller maximum in the resistivity on warming. The cooling curve for the fifth cycle is the source of data represented in Figures 2 and 3. The resistivity in all of the warming curves reached a common resistivity similar to that for the cooling curves

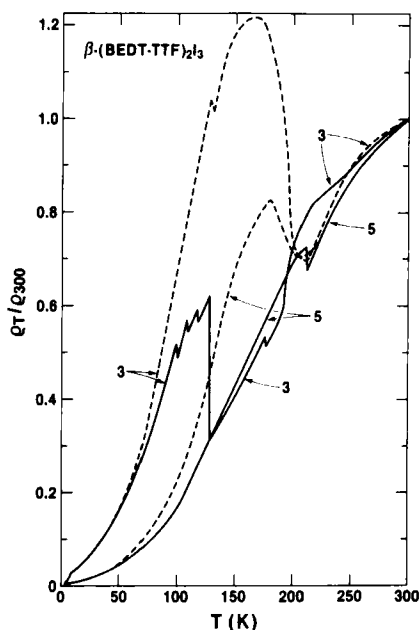


FIGURE 4. Normalized resistivity vs temperature for the thermal cycling of  $\beta$ -(BEDT-TTF) $_2$ I $_3$ . Solid curves are for cooling from 300 K; dashed curves are for warming from 4.2 K. The numbers denote the third (3) and fifth (5) cycles beginning with the initial cooling of a virgin crystal.

at temperatures above  $\sim 230$  K. All of the curves displayed the rapid decrease in resistivity near 8 K. It is interesting to note that if every cooling curve is rescaled at each resistance jump to eliminate the discontinuity, all curves give roughly the same representation of the temperature dependence and the residual resistivity ratio. Our experience suggests that the source of the resistivity jumps is strain developed at the electrical lead-crystal surface interfaces.

After the fifth thermal cycle, the resistivity curves became identical on cooling and warming between 300 K and 150 K. This permitted us to examine the region near 200 K where  $\beta\text{-(ET)}_2\text{I}_3$  undergoes a transition to an incommensurate modulated structure,<sup>8,9</sup> which is the first such structure observed for any organic superconductor. Above 200 K, there is structural disorder in one set of the terminal ethylene groups of the ET cation. Below 200 K, there occurs a modulated superstructure with a modulation wavelength which is incommensurate with the fundamental lattice, and this persists to temperatures at least as low as 10 K. Figure 5 shows the resistivity of the  $\beta\text{-(ET)}_2\text{I}_3$  needle in the region of 280–150 K. The resistivity is

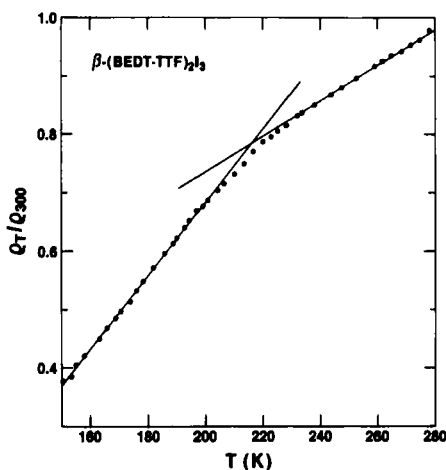


FIGURE 5. Resistivity of  $\beta\text{-(BEDT-TTF)}_2\text{I}_3$  in the region of 280 K – 150 K. The solid lines were derived from a linear least-squares analysis of the plotted experimental points.

linear in  $T$  from 300 K to 230 K, it undergoes a gradual change in slope between 230 K and 200 K, and it again becomes linear in  $T$  with a larger slope at 200 K. There is no evidence of any discontinuity in the resistivity near 200 K. The difference in slopes for the two linear regions, however, is consistent with the possibility that the superstructure represents some long-range ordering which decreases the electron-phonon scattering associated with the high temperature lattice.

ACKNOWLEDGMENT This work was supported by the U.S. Department of Energy, Office of Basic Energy Sciences, Division of Materials Science, under Contract W-31-109-ENG-38.

## REFERENCES

1. D. Jerome, A. Mazaud, M. Ribault, and K. Bechgaard, J. Phys. (Paris) Lett. **41**, L95 (1980).
2. S. S. P. Parkin, E. M. Engler, R. R. Schumaker, R. Lagier, V. Y. Lee, J. C. Scott, and R. L. Greene, Phys. Rev. Lett. **50**, 270 (1983).
3. E. B. Yagubskii, I. F. Shchegolev, V. N. Laukhin, P. A. Kononovich, M. V. Kartsovnik, A. V. Zvarykina, and L. I. Buravov, JETP Lett. **39**, 12 (1984).
4. J. M. Williams, T. J. Emge, H. H. Wang, M. A. Beno, P. T. Copps, L. N. Hall, K. D. Carlson, and G. W. Crabtree, Inorg. Chem. **23**, 2558 (1984).
5. G. W. Crabtree, K. D. Carlson, L. N. Hall, P. T. Copps, H. H. Wang, T. J. Emge, M. A. Beno, and J. M. Williams, Phys. Rev. **B30**, 2958 (1984).
6. L. J. Azevedo, E. L. Venturini, J. E. Schirber, J. M. Williams, H. H. Wang, and T. J. Emge, Mol. Cryst. Liq. Cryst. (in press).
7. H. Schwenk, F. Gross, C.-P. Heidmann, K. Andres, D. Schweitzer, and H. Keller, Mol. Cryst. Liq. Cryst. (in press).
8. P. C. W. Leung, T. J. Emge, M. A. Beno, H. H. Wang, J. M. Williams, V. Petricek, and P. Coppens, J. Am. Chem. Soc. **106**, 7644 (1984).
9. T. J. Emge, P. C. W. Leung, M. A. Beno, A. J. Schultz, H. H. Wang, L. M. Sowa, and J. M. Williams, Phys. Rev. **B30**, 6780 (1984).
10. K. Bender, K. Dietz, H. Endres, H. W. Helberg, I. Hennig, H. J. Keller, H. W. Schafer, and D. Schweitzer, Mol. Cryst. Liq. Cryst. **107**, 45 (1984).
11. F. Behroozi, M. P. Garfunkel, F. H. Rogan, and G. A. Wilkinson, Phys. Rev. **B10**, 2756 (1974).
12. K. D. Carlson, G. W. Crabtree, L. N. Hall, P. T. Copps, H. H. Wang, T. J. Emge, M. A. Beno, and J. M. Williams, Mol. Cryst. Liq. Cryst. (in press).
13. D. U. Gubser, W. W. Fuller, T. O. Poehler, J. Stokes, D. O. Cowan, M. Lee, and A. N. Bloch, Mol. Cryst. Liq. Cryst. **79**, 225 (1982).
14. T. Ishiguro, K. Murata, K. Kajimura, N. Kinoshita, H. Tokumoto, M. Tokumoto, T. Ukachi, H. Anzai, and G. Saito, J. Physique **44**, C3-831 (1983).
15. A. H. Thompson, Phys. Rev. Lett. **35**, 1786 (1975).